

# Sher 25: pulsating but apparently alone

William D. Taylor<sup>1</sup>, Christopher J. Evans<sup>1</sup>, Sergio Simón-Díaz<sup>2,3</sup>, Hugues Sana<sup>4</sup>,  
Norbert Langer<sup>5</sup>, Nathan Smith<sup>6</sup>, Stephen J. Smartt<sup>7</sup>

<sup>1</sup>UK Astronomy Technology Centre, Royal Observatory Edinburgh, Blackford Hill, Edinburgh, EH9 3HJ, UK

<sup>2</sup>Instituto de Astrofísica de Canarias, 38200 La Laguna, Tenerife, Spain

<sup>3</sup>Departamento de Astrofísica, Universidad de La Laguna, Avda. Astrofísico Francisco Sánchez s/n, E-38071 La Laguna, Tenerife, Spain

<sup>4</sup>European Space Agency, Space Telescope Science Institute, 3700 San Martin Drive, Baltimore, MD 21218, USA

<sup>5</sup>Argelander-Unstitut für Astronomie der Universität Bonn, Auf dem Hugel 71, 53121 Bonn, Germany

<sup>6</sup>Steward Observatory, University of Arizona, 933 North Cherry Avenue, Tucson, AZ 85721, USA

<sup>7</sup>Astrophysics Research Centre, School of Maths and Physics, Queen's University Belfast, Belfast BT7 1NN, UK

5 March 2022

## ABSTRACT

The blue supergiant Sher 25 is surrounded by an asymmetric, hourglass-shaped circumstellar nebula, which shows similarities to the triple-ring structure seen around SN1987A. From optical spectroscopy over six consecutive nights, we detect periodic radial velocity variations in the stellar spectrum of Sher 25 with a peak-to-peak amplitude of  $\sim 12 \text{ km s}^{-1}$  on a timescale of about 6 days, confirming the tentative detection of similar variations by Hendry et al. From consideration of the amplitude and timescale of the signal, coupled with observed line profile variations, we propose that the physical origin of these variations is related to pulsations in the stellar atmosphere, rejecting the previous hypothesis of a massive, short-period binary companion. The radial velocities of two other blue supergiants with similar bipolar nebulae, SBW1 and HD 168625, were also monitored over the course of six nights, but these did not display any significant radial velocity variations.

**Key words:** stars: early-type – stars: evolution – stars: individual : Sher 25

## 1 INTRODUCTION

Many of the known Luminous Blue Variable (LBV) stars have associated emission nebulae (e.g. Humphreys & Davidson 1994; Nota et al. 1995). These are thought to have originated from the large amounts of material thrown-off by the parent star during violent episodes of mass-loss. The most famous example is the Homunculus formed by the 19<sup>th</sup> century eruption of  $\eta$  Carinae which, in common with several other LBV nebulae, has a highly bipolar structure.

Observations with the *Hubble Space Telescope* revealed that the progenitor of SN1987A, Sk –69°202 (classified as B0.7-3 I by Walborn et al. 1989), was surrounded by a bipolar nebula that pre-dated the supernova explosion by about 20,000 years (Burrows et al. 1995a). This comprises a well-defined equatorial ring and two larger rings that are roughly plane-parallel with the inner ring but offset along the system's polar axis (see Figure 1). Indeed, the similarity of the nebula around SN1987A to that seen around the candidate LBV HD 168625, led Smith (2007) to suggest that Sk –69°202 may have been a low-luminosity quiescent LBV, or that it had at least undergone an LBV-like eruption in its recent past.

The LBV candidate Sher 25 is a B-type supergiant

slightly to the northeast of the young massive cluster NGC 3603 (Sher 1965); classified as B1.5 Iab (Moffat 1983). It too has an associated nebula, consisting of a well-defined central ring with two asymmetric lobes of material on either side (Brandner et al. 1997b, see Figure 1). The similarities in their spectral types and associated nebulae have led to comparisons of Sher 25 with SN1987A (e.g. Brandner et al. 1997a; Smartt et al. 2002).

There is no clear consensus as to how the ring structures surrounding these stars were formed. One of the most successful models is that of a binary merger between a  $15 M_{\odot}$  star and a  $5 M_{\odot}$  companion (Morris & Podsiadlowski 2009). Alternatively, Chita et al. (2008) argued that a single star could generate this complex structure through the interaction of its stellar wind with material deposited during earlier stages of the star's evolution. Both of these models require the star to have passed through a red supergiant (RSG) phase, whereas a more recent theory by Smith et al. (2013) is independent of previous evolutionary stages. In this model the equatorial ring has been formed in a previous unexplained mass-loss event, while the subsequent photoevaporation of material from this ring interacting with the stellar wind forms the polar rings. Whether the progenitor

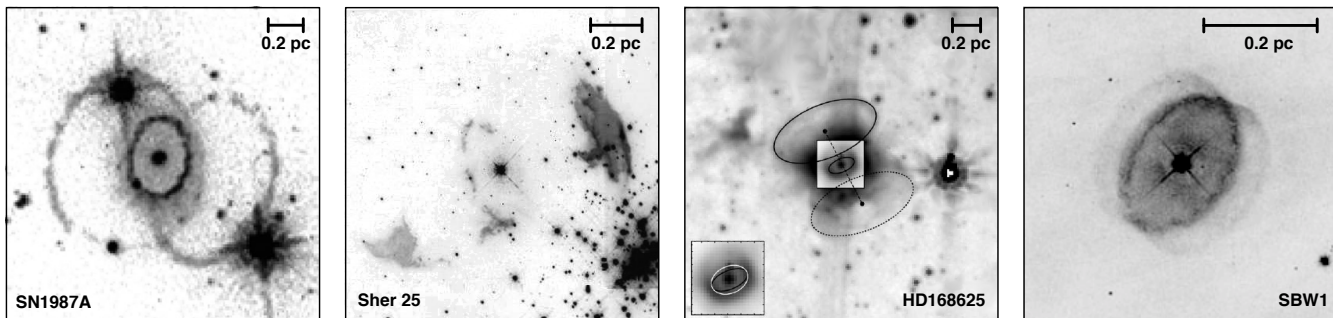


**Figure 1.** Images of the famous triple-ring nebula of SN1987A and the three LBV candidates observed in this study. SBW1 also has three well-defined rings making it the closest analogue of SN1987A, while Sher 25 has large lobes of material aligned along the axis of the central ring. The rings of HD 168625 are faint, so have been highlighted in this *Spitzer* image from Smith (2007). Other image credits: SN1987A, *HST*, Burrows et al. (1995b); Sher 25, *HST*, Brandner et al. (1997b); and SBW1, *HST*, Smith et al. (2013).

of SN1987A and Sher 25 have passed through a RSG phase cannot currently be determined conclusively.

In the course of investigating the abundances of Sher 25 and its nebula, Hendry et al. (2008) detected radial velocity (RV) shifts with peak-to-peak amplitude of  $\sim 12 \text{ km s}^{-1}$  from the five stellar observations available. The RV shifts were consistent with either a three or six day period of a binary companion. Hendry et al. noted that the implied secondary in such a scenario would have to be more massive than Sher 25 itself, and yet we see no evidence for such a companion - for instance, Nazé et al. (2012) found no significant X-ray emission from Sher 25, which might be expected if a massive short-period companion were present. Hendry et al. speculated that a binary with a centre-of-mass within the radius of Sher 25 might account for the observations (i.e. a slow merger), but also noted that the RV shifts may have arisen from pulsations or some other process in the stellar envelope. Indeed, their reported RV shifts were roughly the same magnitude as their measurement uncertainties, although no equivalent shift was seen in the interstellar Ca II absorption suggesting that the signature was real.

If Sher 25 has a short-period binary companion it could have important consequences for our understanding of the formation of its nebula. Likewise, the presence and type of pulsations within the stellar atmosphere could potentially indicate different evolutionary histories (Saio et al. 2013). Here we report on a comprehensive set of follow-up observations to investigate the nature of Sher 25 in more depth.

We also report on observations of two other LBV candidates with similarities to SN1987A and Sher 25, namely HD 168625 (e.g. Smith 2007) and SBW2007 1, commonly known as SBW1 (Smith et al. 2007). Both are also surrounded by triple-ring structures (see Figure 1). Classified as B6 Iap (Walborn & Fitzpatrick 2000), HD 168625 has a luminosity comparable to that estimated for Sk  $-69^{\circ}202$ , while Smith et al. (2013) argue that the nebula of SBW1 is the closest known analog to that of SN1987A.

## 2 OBSERVATIONS

The three stars were observed over six consecutive nights (spanning March 19-24<sup>th</sup> 2009) using FEROS on the Max Planck Gesellschaft (MPG)/European Southern Observa-

tory (ESO) 2.2-m telescope at La Silla. FEROS is a fixed-configuration instrument, with a wide wavelength coverage of  $\lambda\lambda 3600\text{--}9200 \text{ \AA}$  at a spectral resolving power of 48 000. Sher 25 and SBW1 are sufficiently faint ( $V = 12.3$  and 12.7, respectively) that pairs of back-to-back exposures of 2400 s were obtained. HD 168625 ( $V = 8.4$ ) was observed in a series of shorter back-to-back exposures (of 240 to 600 s). A full list of the observations is given in Table A1.

The data were reduced using the ESO Data Reduction Software pipeline for FEROS. Further steps can be taken beyond the pipeline reductions to improve the merging of the spectral orders, but this was not necessary for our purposes. Also, our targets are sufficiently bright that the spectrum from the FEROS sky fibre was not subtracted; indeed, subtraction of the sky fibre actually degraded our data given the additional source of noise.

Cosmic rays were removed from the individual spectra via comparisons with a median-averaged spectrum of all the observations of each star. The flux ratio of each spectrum to the median was calculated and a boxcar  $5\sigma$ -clip was applied over 100 wavelength bins to identify and remove likely cosmics. Note that the median-averaging of the spectra means that significant RV shifts in spectral lines between frames could lead to regions being flagged as ‘suspect’ pixels. Thus, only suspect pixels which were  $5\sigma$  greater than the local continuum were removed, ensuring that any absorption features were preserved intact.

The cleaned spectra were rectified by division of a low-order polynomial fit to the continuum. Back-to-back exposures of Sher 25 and SBW1 were coadded to increase the signal to noise ratio (S/N), while all of the exposures of HD 168625 from a given night were coadded together as they were obtained in quick succession. The typical S/N achieved in the final spectra (measured around  $\lambda 4560 \text{ \AA}$ , in the middle of the Silicon triplet) was  $\sim 50$  for Sher 25 and SBW1, and  $\sim 120$  for HD 168625; example spectra of are shown in Figure 2. The ratio of the Si IV to Si III lines suggest that SBW1 is marginally hotter than Sher 25, which is also suggested by the presence of He II  $\lambda 4686$  in SBW1’s spectra. We therefore propose that SBW1 is reclassified as B1 Iab, while Sher 25 retains its original classification of B1.5 Iab from (Moffat 1983), noting the slight disagreement with Melena et al. (2008), who classified Sher 25 as B1 Iab.

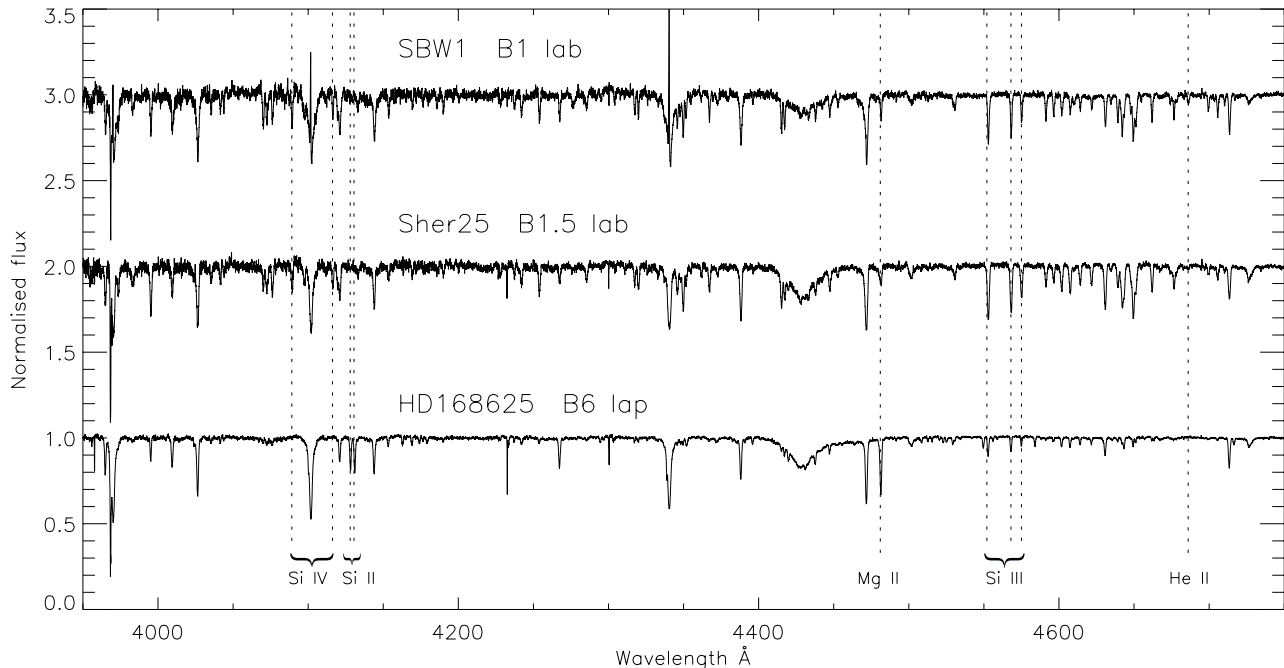


**Figure 2.** The blue-visual region of the median spectra of the three B-type supergiants observed with FEROS. For clarity the spectra have been smoothed using a 5-pixel, boxcar rolling average. The dashed lines indicate some of the most temperature sensitive lines for B-type supergiants.

## 2.1 Radial velocity measurements

Estimated RVs for each spectrum were obtained from two different methods: profile fitting of sets of absorption lines and cross-correlation (of sub-sections) of the spectra from different epochs. In estimating the RVs, different regions were employed from the broad coverage of the FEROS observations to ensure that any measured signal was derived from different spectral orders (reducing the possibility that an observed signal could be instrumental in origin). Also, lines from a number of different atomic species were used in the analysis, a full list of which is given in Table A1.

Prior to profile fits, a localised correction of the continuum rectification was undertaken for each selected line using small regions on either side of the absorption profile. The selected lines were fit in the median-averaged spectrum initially. This defined a median width and depth of each line, which could then be held constant for the fits to the individual (noisier) spectra, thus improving the precision of the resulting RV estimates. For a number of lines the S/N was low and so not all lines were included in the final analysis, as indicated in Table A1 at the end of the paper.

As an independent check on the line-fitting analysis, measurements were also made using cross-correlation techniques. Three spectral regions were selected, each of which contained well-resolved absorption lines available for inter-comparison:  $\lambda\lambda 4500\text{-}4700$ ,  $\lambda\lambda 5650\text{-}5750$  and  $\lambda\lambda 8580\text{-}8680$  Å.

The relative RV measurements for HD 168625 and SBW1 are shown in Figure 3, with those for Sher 25 in Figure 4; the full set of measurements is recorded in Table A1. A clear RV variation is present in the Sher 25 results from both the profile fits and from the cross-correlation analysis.

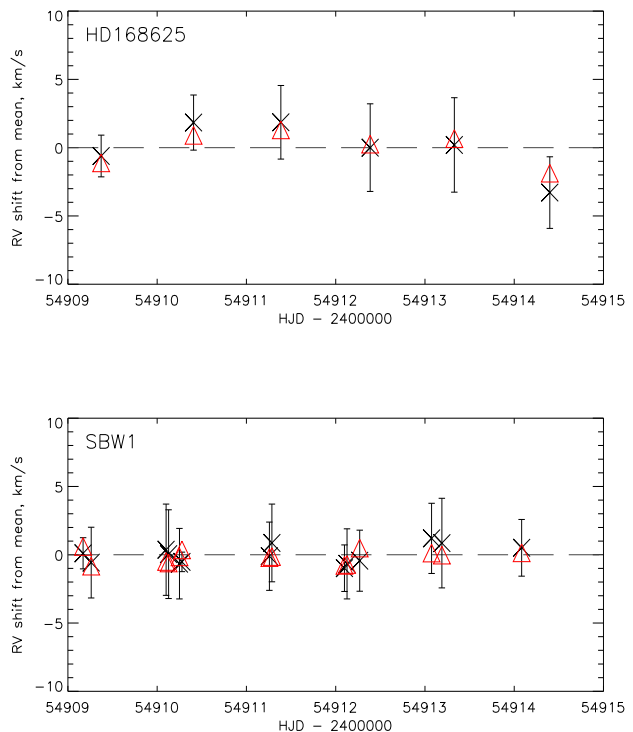


**Figure 3.** Radial velocity measurements for HD 168625 and SBW1. Black crosses: mean RV shifts estimated from Gaussian fits to spectral lines (with the  $1\sigma$  standard deviations indicated by the error bars). Red triangles: mean shifts estimated from cross-correlation measurements of the selected regions of the data.

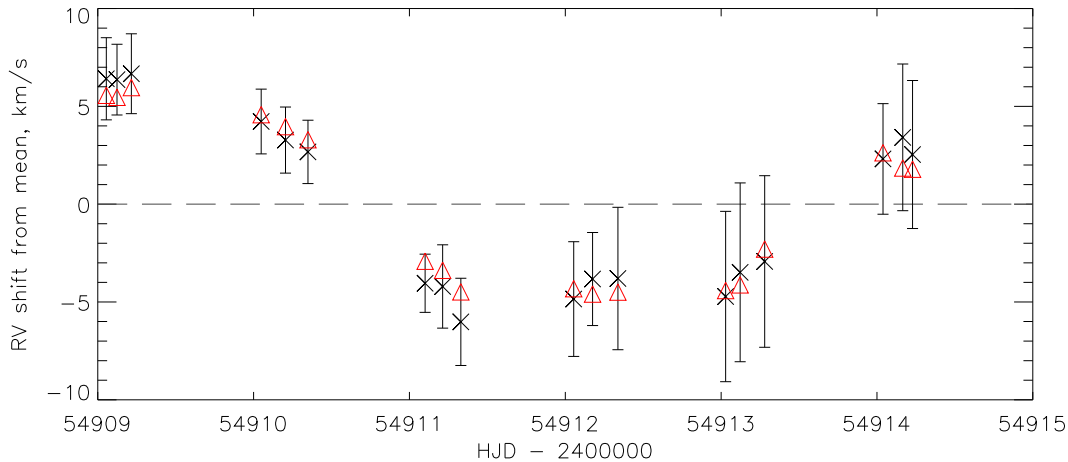


**Figure 4.** Radial velocity measurements for Sher 25. The symbols have the same meaning as those used in Figure 3.

**Table 1.** Measured RV shifts for previous FEROS observations of Sher 25. The mean shifts use the same zero-point as the values listed in Table A1.

Date (HJD - 240000)	Mean RV shift (km s <sup>-1</sup> )	Error (km s <sup>-1</sup> )
51327.000	3.20	6.00 <sup>a</sup>
53191.092	-3.81	3.63
53193.054	2.36	3.81
53369.852	3.17	3.24
53370.852	-7.62	3.06
53371.828	-8.15	2.58

<sup>a</sup> For this epoch the measured value and error are from Hendry et al. (2008) adjusted to the same zero-point as the other epochs.

The magnitude of the RV variations is consistent with that reported by Hendry et al. (2008), but due to the delay since the previous observations, no attempt was made to include them in the period searches.

Qualitative inspection of the results for HD 168625 suggest a weak trend with time (upper panel of Figure 3), but any deviation is within the associated uncertainties so we are unable to draw firm conclusions from the current data. We find no evidence for significant short-term variations in SBW1 (lower panel of Figure 3).

### 3 INTERPRETATION OF RV SHIFTS

In the following sections we consider possible scenarios to explain the apparent RV variations detected in Sher 25’s spectra. We begin by investigating binary companions as this was the initial motivation for this study. However, we note that the amplitude of the detected variations is modest, particularly in light of results for B-type supergiants in Westerland 1 from Ritchie et al. (2009), who found  $\Delta RV = 15\text{--}25 \text{ km s}^{-1}$  for some of their targets for which they were unable to distinguish between orbital and photospheric effects.

#### 3.1 Credible companions?

An estimate of the periodic timescale for the RV signal was found from a basic Fourier analysis to be  $\sim 6$  days. Initial inspection of the data might suggest that the observed RV shift could represent the peak of a longer, larger oscillation: however, testing showed that the first night’s observations constrain the fit to this apparent 6-day timescale. While caution should be exercised when assuming the observed variation is truly periodic, in the analysis that follows we consider the impact of these RV signals as if they were a periodic pattern - an assumption that is tentatively supported by the similarities to previous observations (see Table 1).

The 6-day period was used as the initial input to the Liège Orbital Solution Package (see Sana et al. 2006), to fit an orbital solution to the data assuming that Sher 25 is an elliptical SB1 system (using the well-established techniques of Wolfe et al. 1967). The salient parameters from this fit being a putative period of  $6.1 \pm 0.7$  days with an amplitude of  $6.12 \pm 0.28 \text{ km s}^{-1}$ . Note that it is not possible to constrain the period more tightly as the timebase of the observations is comparable to the apparent period.

From comparisons of their model atmosphere results with the evolutionary tracks of Meynet et al. (1994), Hendry et al. estimated the present-day mass of Sher 25 to be  $40 \pm 5 M_{\odot}$  with a radius of  $60 \pm 15 R_{\odot}$ . Adopting this mass estimate for the primary, assuming an inclination of  $65^{\circ}$  from the measured tilt of the central ring (Brandner et al. 1997b) and using the results from the orbital fit, results in an estimated secondary mass of  $\approx 0.66 \pm 0.2 M_{\odot}$ . This contrasts with the suggested high-mass companion of Hendry et al. (2008) as we have measured a longer period.

Following Keplerian arguments the orbital separation of the two hypothetical components is calculated to be  $\sim 40 \pm 14 R_{\odot}$ ; i.e. a companion would be very close to, or even within, the extended envelope of the primary. Similar calculations with the primary mass varied by up to  $\pm 50\%$  (i.e. allowing for different evolutionary scenarios where Sher 25 may have passed through a RSG phase), also suggest a low-mass companion at a separation comparable to the estimated radius of the primary. It therefore seems unlikely that the observed RV signal is the result of a binary companion.

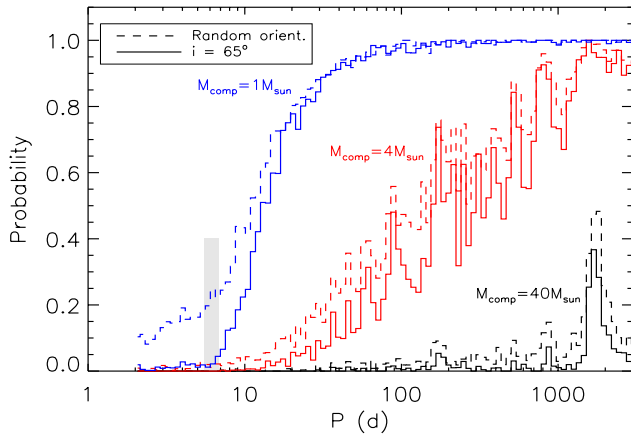


**Figure 5.** Probability that a possible companion around Sher 25 would generate a RV signal smaller than the detection threshold for these observations. The shaded band indicates the predicted 6.1 day period and its associated error.

### 3.1.1 Other possible binary companions

It is interesting to explore the orbital properties and companion mass that would be compatible with the RV signal detected for Sher 25. To do this we used the methods of Sana et al. (2009, 2011) to simulate the observable RV shifts that would be expected for various binary systems. Three different mass-ratios were modelled, each with a  $40 M_{\odot}$  primary and either a  $40 M_{\odot}$ ,  $4 M_{\odot}$  or  $1 M_{\odot}$  secondary. A range of orbital eccentricities consistent with those of Sana et al. (2012) were considered. Predictions can then be made about the probability of detecting the expected RV shifts assuming the typical error of our measurements and the time-sampling of the observations. To further increase this time-sampling, the previous FEROS observations from Hendry et al. (2008) were re-analysed using the methods described above (for completeness, the measured RV shifts of these additional observations are detailed in Table 1). Figure 5 shows the probability results for the three different mass-ratios and also the impact of assuming an inclination for the system of  $65^{\circ}$ , as measured by Brandner et al. (1997b). The probabilities represent confidence levels of  $4.7\sigma$ , which equate to velocity shifts of  $15 \text{ km s}^{-1}$ .

Figure 5 confirms that the properties of the RV signal detected (both RV amplitude and timescale) cannot be reproduced by a physically realistic companion. It is possible that one or even several companions exist beyond our detection threshold, i.e. at orbital separations large enough to produce a negligible signal in our data. Searching for such companions would require either long-term spectroscopic monitoring or very high-angular resolution techniques (Sana et al 2014, ApJS, *subm.*). The impact of such putative companions on the evolution of Sher 25 would then depend on the companion’s mass, eccentricity and orbital separation.

## 3.2 Wind variability?

Hendry et al. (2008) commented on variations in Sher 25’s H $\alpha$  P-Cygni wind profile and similar variations are present in the new FEROS data (see the upper panel of Figure 6). This behaviour could be caused by inhomogeneous large-

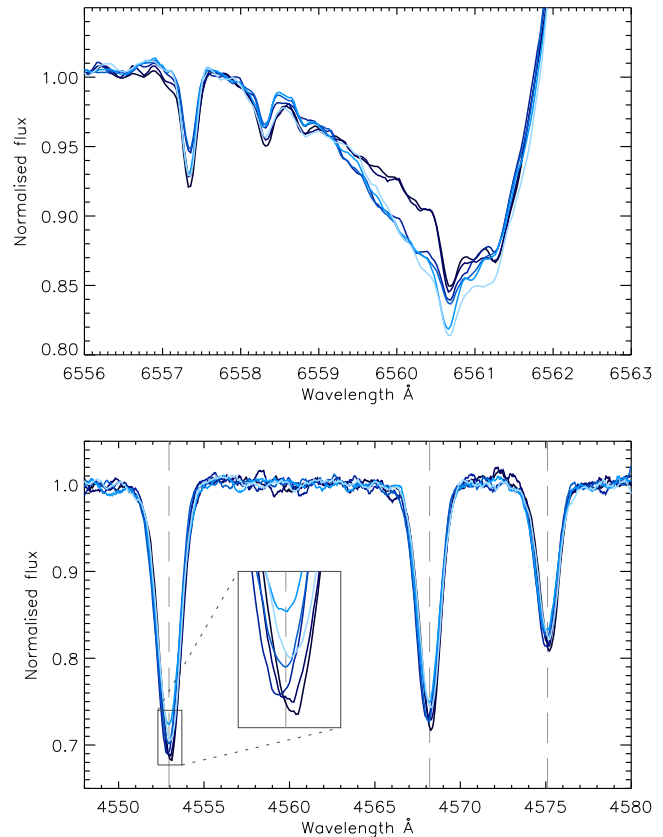


**Figure 6.** The upper panel shows the variation in the wind profile of the H $\alpha$  line for Sher 25, while the lower panel shows the subtle changes in the profile shapes of the Si III triplet. The colour indicates the observation’s date, going from black to cyan (i.e. dark to light) with increasing time. For clarity, the data from each night have been coadded and smoothed using a 5-pixel boxcar average.

scale structure within the wind, leading to variations in the absorption profile (e.g., Markova et al. 2005). The H $\alpha$  profiles do not display periodic behaviour within our observations, and although the similarity with the previous data might suggest some longer period repeatability, it is clearly with a different timescale to the observed RV shifts. Wind variability is therefore unlikely to be the origin of Sher 25’s apparent RV signal.

## 3.3 Possible pulsations?

A number of Sher 25’s metal lines appear to show small-scale variations. Such behaviour is seen in many OB-supergiants and has long been attributed to pulsations within the stellar envelope (Lucy 1976). The lower panel of Figure 6 shows the variation in depth seen for the Si III triplet of Sher 25. There is a less obvious trend with time than in the H $\alpha$  profile – the deepest profiles are from the first night, with the lines appearing to get shallower until the final night, when the pattern reverses, hinting at a more periodic behaviour.

Balona (1986) proposed that the temporal variation of the first three moments of a line-profile could be used to investigate pulsations in stars. Specifically, the first moment provides a measurement of the centroid velocity, and

the third moment (‘skewness’) gives a measurement of any asymmetry in the lines. Following this strategy, one can better separate real RV variations, e.g. due to binarity, from those resulting from pulsations, i.e. when the line centre is ‘wobbling’ due to changes in the skewness and, consequently, the measured velocity of the line also appears to move.

Through the FAMIAS<sup>1</sup> package (Zima 2008), which employs the moment analysis techniques of Briquet & Aerts (2003), we computed the third moment of all the Si III triplet lines (lower panel of Figure 6). The results are shown in Figure 7 and clearly suggest that there is periodic variation in the skewness of the lines, with a period similar to the measured RV variations. The order of magnitude and the time frame of these variations are consistent with those observed for other B-type supergiants by Simón-Díaz et al. (2010), although the pattern is noticeably more periodic than the stars of described therein. It is possible that the relatively long exposures used for Sher 25 have smoothed out possible smaller-scale variations. Our hypothesis is therefore that the observed RV variations in Sher 25 are the result of line profile variations arising from stellar pulsations.

Similar skewness tests were performed for SBW1 and HD 168625, with neither showing a variation in the skewness results compared to that for Sher 25. This is consistent with the lack of detected RV variation in these two stars. Of course, this cannot rule out the presence of any undetected longer period variations for these stars.

To assess the type of pulsation seen in Sher 25, V-band photometric data were obtained from ASAS<sup>2</sup> to look for brightness variations that would imply radial pulsations. The ASAS data revealed no significant variation: indeed the standard deviation of the measurements was  $<0.03$  mag, which is comparable with the anticipated error on the ASAS measurements. Searches revealed no periodic signatures consistent with the predicted  $6.1 \pm 0.7$  day period. As an additional check, the Baade-Wesselink method can be used to estimate the typical RV-shifts associated with brightness variations. For a star with the properties of Sher 25 and assuming a 6 day period, a 0.03 mag variation would be expected to induce a RV-shift of  $<2$  km s<sup>-1</sup>. We can therefore conclude that the observed RV signal of Sher 25 is not associated with radial pulsations.

### 3.3.1 Macroturbulence

The line profiles of many luminous B-type stars cannot be accurately described simply by rotational broadening, an additional broadening mechanism - so called ‘macroturbulence’ - must be invoked. Aerts et al. (2009) showed that the observed profiles could be generated through the superposition of numerous low-amplitude non-radial gravity mode oscillations within the stellar envelope. They predicted that the magnitude of this contribution should be proportional to any variation in the profile skewness, a result that has since been verified observationally by Simón-Díaz et al. (2010).

We calculated the macroturbulent velocity ( $\Theta_{RT}$ ) of

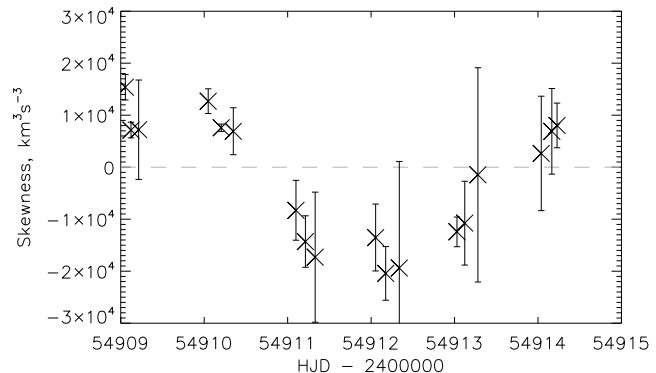


**Figure 7.** Skewness results for Sher 25. The data show the mean skewness for each observation calculated from the Si III triplet. The errors represent the standard deviation on the measurements of the three lines.

all the stars using the techniques of Simón-Díaz & Herrero (2014), which exploits a combined Fourier transform and goodness of fit technique to disentangle the broadening contributions from rotation and macroturbulence. The results of the analysis are shown in Table 2. For Sher 25 the magnitude of these broadening terms and the results of the skewness analysis above, are consistent with both the predictions of Aerts et al. (2009) and the measurements of Simón-Díaz et al. (2010), suggesting that in this respect, Sher 25 is similar to other pulsating B-type supergiants.

The  $\Theta_{RT}$  estimate for SBW1 is not that much lower than that for Sher 25; therefore, based on the predictions of Aerts et al. (2009), we would have expected to find some evidence of skewness variation for SBW1. It is possible that the time-sampling of the observations is insufficient to detect the variation or that the signal has been smoothed out by the relatively long exposures. Understanding the relationship between pulsations and line broadening is still in its infancy; these results suggest that the frequency of pulsations will also prove an interesting area to explore further.

### 3.3.2 Evolutionary implications of pulsations

Through modelling crossed-checked against observations, it is possible to define evolutionary phases when supergiants are more likely to undergo pulsations. Pamyatnykh (1999) defined the regions in which stars might experience high-order g-mode instabilities, and later Saio et al. (2006) identified a region of stars exhibiting Post-TAMS low-order g-mode oscillations. The results of the FASTWIND analysis for Sher 25 performed by Hendry et al. (2008), suggest that the star lies on the boundary of these two instability regions; it is therefore not surprising that the star exhibits pulsations.

Saio et al. (2013) have taken these ideas further to argue that the evolutionary history of a star could be unravelled by the type of pulsation it exhibits. They argue that if a blue supergiant displays evidence for radial pulsations and lies within a certain region of the Hertzsprung-Russell Diagram (HRD), then it must have passed through a previous RSG phase and is currently on a blue-loop travelling back across the HRD. Unfortunately it is not possible to use these techniques to better understand Sher 25’s history as it lies

<sup>1</sup> FAMIAS was developed in the framework of the FP6 European Coordination Action HELAS (<http://www.helas-eu.org/>)

<sup>2</sup> The ‘All Sky Automated Survey’ provides constant photometric monitoring for all objects with  $V < 14$  mag (Pojmanski 1997).

**Table 2.** Rotational and macroturbulent velocities derived from a combined Fourier transform and goodness of fit technique.  $v_{eq}$  gives an estimate for the stars’ equatorial velocities based on inclinations derived from the central ring of the nebulae (see text for references). The quoted errors reflect the  $3\sigma$  confidence region of the fit and all the quoted velocities are in  $\text{km s}^{-1}$ .

Star	$v \sin i$	$\Theta_{RT}$	$v_{eq}$
Sher 25	53 (+11/-8)	72 (+13/-11)	64 (+13/-10)
SBW1	34 (+23/-15)	55 (+21/-17)	41 (+28/-18)
HD168625	44 (+6/-8)	44 (+16/-16)	53 (+7/-10)

just outside Saio’s identified region and the absence of any significant photometric variation suggests that it does not exhibit radial pulsations. For SBW1, however, the luminosity and temperature estimates of Smith et al. (2013) suggest that the star lies within Saio’s identified region, and while in no way conclusive, the absence of any pulsations for SBW1 supports the argument that the star has not passed through an RSG phase (Smith et al. 2013).

#### 4 DISCUSSION

It is interesting to consider whether the results reported here can influence the debate on the origin of the nebulae that surround these three stars and SN1987A.

While no binary companions were found in this study, the estimates for detection probabilities of other companions presented in Figure 5 indicate that it is quite possible that a smaller companion with a longer period could have gone undetected. Although, it should be noted that the entire lifetime of a B1 supergiant is comparable to the pre main-sequence lifetime of a solar-mass star. Therefore, if a small companion does now exist, it must have started life with a higher mass and subsequently had mass stripped from it, a process that would have significantly affected the evolution of both stars.

If at a later date any companion were discovered, our analysis would suggest that it will either be a distant one, which may have had little impact on Sher 25’s evolution, or a small nearby companion, which has undergone significant interaction with Sher 25. Frustratingly, this therefore does little to influence the nebula-origin debate.

Our treatment of macroturbulence has led to a lower estimate of the rotational velocity of  $58 \text{ km s}^{-1}$  compared to the previous estimate of  $108 \text{ km s}^{-1}$  from Smartt et al. (2002) - again this is assuming the inclination from Brandner et al. (1997b). The rotational velocity of these stars is of particular relevance, as it could help assess the likelihood of different models. As an example, Smith & Townsend (2007) express concern that the binary merger model of Morris & Podsiadlowski (2009) has insufficient time to slow the star’s rotation since the merger. This problem is exaggerated by the slower  $v \sin i$  estimates reported here.

Interestingly, Heger & Langer (1998) predicted that a single  $25 M_{\odot}$  star would deposit material in an equatorial ring as it began a blue-loop back across the HRD following a RSG phase. Their models predicted that the star’s rotation would be dramatically slowed as angular momentum would

be lost to the material deposited in the ring. They estimated that the final rotational velocity of the star would be around  $50 \text{ km s}^{-1}$ , which is intriguingly close to that found for the stars in this study. This type of mechanism, coupled with the polar rings of Smith et al. (2013) that are formed through photoevaporation of material from the equatorial ring, could provide a possible solution for forming these nebula.

A final consideration is whether the stars have passed through a RSG phase. This is necessary for the models of Heger & Langer (1998), but for SBW1 the surface abundances suggest this is not the case - a conclusion which is tentatively supported by the pulsational theories of Saio et al. (2013) discussed above. Interestingly Georgy et al. (2013) have expanded on Saio’s work to show that through different modelling techniques a star could be seen to have lower than expected surface abundances even after passing through a RSG phase. This opens again the question of SBW1’s history and shows that this crucial debate surrounding the possible RSG phase of these stars appears to be far from solved.

#### 5 CONCLUSION

Due to its similarities to the mysterious SN1987A, Sher25 is an excellent example of a very interesting breed of stars. This work strongly suggests that the star is pulsating in a regular periodic way, which mimics the RV signal of a small binary companion. Such a companion is believed to be unlikely because the variation in the skewness of the line profiles matches the period of the RV shifts, and also because any binary system with these orbital parameters would be relatively unphysical. This work therefore lays to rest the possibility of a massive short-period companion raised by Hendry et al. (2008).

Both SBW1 and HD168625 appear to show no evidence for either RV variations or pulsations on the timescales of a few days considered here. All three stars are found to exhibit macroturbulent line-broadening, which lowers some of the previous estimates for their rotational velocity. These new estimates of rotation should provide additional constraining factors in the simulations of those seeking to explain the origin of these extraordinary nebulae.

ACKNOWLEDGEMENTS: Based on observations at the European Southern Observatory primarily from programme 082.D-0136, but with additional analysis of observations from 071.D-0180 and 074.D-0021. With thanks to Selma de Mink for useful discussions about possible (or in fact, not possible) binary scenarios. SS-D acknowledges funding by the Spanish Ministry of Economy and Competitiveness (MINECO) under the grants AYA2010-21697-C05-04, Consolider-Ingenio 2010 CSD2006-00070, and Severo Ochoa SEV-2011-0187, and by the Canary Islands Government under grant PID2010119. SJS thanks the ERC and EU’s (FP7/2007-2013)/ERC Grant agreement n° [291222].

#### REFERENCES

Aerts C., Puls J., Godart M., Dupret M.-A., 2009, *A&A*, 508, 409  
 Balona L. A., 1986, *MNRAS*, 219, 111

- Brandner W., Chu Y.-H., Eisenhauer F., Grebel E. K., Points S. D., 1997a, *ApJ*, 489, L153
- Brandner W., Grebel E. K., Chu Y.-H., Weis K., 1997b, *ApJ*, 475, L45
- Briquet M., Aerts C., 2003, *A&A*, 398, 687
- Burrows C. J. et al., 1995a, *ApJ*, 452, 680
- Burrows C. J. et al., 1995b, *ApJ*, 452, 680
- Chita S. M., Langer N., van Marle A. J., García-Segura G., Heger A., 2008, *Astronomy and Astrophysics*, 488, L37
- Geogy C., Saio H., Meynet G., 2013, *MNRAS*
- Heger A., Langer N., 1998, *A&A*, 334, 210
- Hendry M. A., Smartt S. J., Skillman E. D., Evans C. J., Trundle C., Lennon D. J., Crowther P. A., Hunter I., 2008, *MNRAS*, 388, 1127
- Humphreys R. M., Davidson K., 1994, *PASP*, 106, 1025
- Lucy L. B., 1976, *ApJ*, 206, 499
- Markova N., Puls J., Scuderi S., Markov H., 2005, *A&A*, 440, 1133
- Melena N. W., Massey P., Morrell N. I., Zangari A. M., 2008, *AJ*, 135, 878
- Meynet G., Maeder A., Schaller G., Schaerer D., Charbonnel C., 1994, *A&AS*, 103, 97
- Moffat A. F. J., 1983, *A&A*, 124, 273
- Morris T., Podsiadlowski P., 2009, *MNRAS*, 399, 515
- Nazé Y., Rauw G., Hutsemékers D., 2012, *A&A*, 538, A47
- Nota A., Livio M., Clampin M., Schulte-Ladbeck R., 1995, *ApJ*, 448, 788
- Pamyatnykh A. A., 1999, *Acta Astron.*, 49, 119
- Pojmanski G., 1997, *Acta Astron.*, 47, 467
- Ritchie B. W., Clark J. S., Negueruela I., Crowther P. A., 2009, *A&A*, 507, 1585
- Saio H., Geogy C., Meynet G., 2013, *MNRAS*, 433, 1246
- Saio H. et al., 2006, *ApJ*, 650, 1111
- Sana H. et al., 2012, *Science*, 337, 444
- Sana H., Gosset E., Evans C. J., 2009, *MNRAS*, 400, 1479
- Sana H., Gosset E., Rauw G., 2006, *MNRAS*, 371, 67
- Sana H., James G., Gosset E., 2011, *MNRAS*, 416, 817
- Sher D., 1965, *MNRAS*, 129, 237
- Simón-Díaz S., Herrero A., 2014, *A&A*, 562, A135
- Simón-Díaz S., Herrero A., Uytterhoeven K., Castro N., Aerts C., Puls J., 2010, *ApJ*, 720, L174
- Smartt S. J., Lennon D. J., Kudritzki R. P., Rosales F., Ryans R. S. I., Wright N., 2002, *A&A*, 391, 979
- Smith N., 2007, *AJ*, 133, 1034
- Smith N., Arnett W. D., Bally J., Ginsburg A., Filippenko A. V., 2013, *MNRAS*, 429, 1324
- Smith N., Bally J., Walawender J., 2007, *AJ*, 134, 846
- Smith N., Townsend R. H. D., 2007, *ApJ*, 666, 967
- Walborn N. R., Fitzpatrick E. L., 2000, *PASP*, 112, 50
- Walborn N. R., Prevot M. L., Prevot L., Wamsteker W., Gonzalez R., Gilmozzi R., Fitzpatrick E. L., 1989, *A&A*, 219, 229
- Wolfe, Jr. R. H., Horak H. G., Storer N. W., 1967, *The machine computation of spectroscopic binary elements*, Gordon & Breach, p. 251
- Zima W., 2008, *Communications in Asteroseismology*, 157, 387

